

## ABSORPTION DEGRADATION OF MONO-Si AND POLY-Si SOLAR CELLS DUE TO HOT SPOT FORMATION

G. O. OSAYEMWENRE\*, E. L. MEYER

*Fort Hare Institute of Technology (FHIT), University of Fort Hare, South Africa*

This paper focuses on the absorption degradation of solar cells absorbance due to localized heat. We investigated the reduction in Mono-Si and Poly-Si solar cell absorption and correlated this with hot spot formation. Fourier Transform Infrared Spectroscopy (FTIR) was used for the absorption characterization. In investigating the susceptibility of these cells to hot spot formation, an artificial method was employed to create defects, by subjecting the device to a reverse biased condition. This method was chosen to deduce a practical effect of hot spot formation on these cells' absorption power. Results showed that there was a decrease in the optical density of these solar cells after defect formation when both the affected and non-affected region were compared. A decrease in optical absorbance represents a huge problem because of the long-term solar cell degradation, as well as a decrease in absorption coefficient and a reduction in solar cell conversion efficiency. This decreases the photo-generating current hence reduces the efficiency of the solar device. These results show a direct correlation between localized heat and absorption degradation, at certain wave number the percentage loss of the incident photon was up to 91% and 81% for Mono-Si and Poly-Si respectively.

(Received July 6, 2014; Accepted September 24, 2014)

*Keywords:* Spectroscopy, Photovoltaic (PV), Hot spot, degradation, Absorbance.

### 1. Introduction

Throughout the history of solar cell development, an efficiency increase has been a major priority because a low efficiency is one of the chief disadvantages in Photovoltaic (PV) industries [1-3]. Such improvement includes the development of a better model for increasing the absorbance of the solar device. The principle lies in, maximizing the number of photons of the right frequency reaching the active layer of the cell. Once this is achieved, it helps boost the photo-generated current. There are numerous published documents on the limitations of PV technologies as an alternative energy source to the already strained grid electricity. Ninety percentages of such works identify low efficiencies as the primary limiting factor for PV cells [5], while ten percentages is on current-loss mechanisms. A detailed account was presented by Hirst on the concept of the solar cell loss process [6]. Recognizing the primary loss mechanism in solar cells enables future studies to focus on how to cut down or do away with these detected losses [6-7]. The present work acknowledges absorption degradation as another loss mechanism from a solar cell.

This article, considers the absorption capability of two PV technologies. When incident light falls upon the surface of PV cells, the absorption of photons of energy greater than the band gap occurs. Solar cell absorption coefficient depends on the intrinsic layer concentration of the cell; this layer can be affected by the presence of localized heating, as such minimize the useful photon [6-7]. Depletion in the quantity of the incident photon absorbed automatically diminished the photo-generated current.

The present paper investigated the effect of hotspot formation on the absorption coefficient of solar cells. It is generally assumed that the optical properties of the various layers in

---

\*Corresponding author: gosayemwenre@ufh.ac.za

PV cell are conserved during operation. Research shows that modules do degrade when deployed outdoor [8]. Moreover, optical degradation contributes to the net degradation of PV cells/modules hence there is a direct correlation between efficiency and optical degradation.

The absorbance of a device is the indicative of the quantity of photons it can absorb. With the aid of the absorption coefficient, PV solar cells are able to transmit electromagnetic energy to electrical energy through the internal energy of the absorber layer [9-11]. One limitation of light passing into a material medium is the decrease in its absorption capacity. There are several factors responsible for this decrease. Some of these relate to the type and thickness of the material medium, the surface morphology (structural damage), optical density (absorbance) and the absorption coefficient. The absorption power of PV cells depends on: the absorption coefficient, penetration depth, material absorbance (optical density) and the percentage of the incident light absorbed.

## 2. Experimental details

### 2.1 Induction of defect

Three Multi-Si and three Mono-Si cells were subjected to a comprehensive visual inspection. This was done to detect possible visible defects. Interestingly, no visual defect was found. The next step involved the creation of defect (hot spot). This was done through the reverse bias process. The aim of this process was to induce defects in the device, so that regions of higher impurities can develop hot spots. Regions of high impurities in solar cells are prone to defect formation (hot spot) when short circuited or reverse biased for a longer period of time [12], this procedure corresponds to the IEC 2005 assessment procedure.

The Hantel programmable high-precision lab bench DC power supplier, which is a variable power supply, was used to supply 12 volts and 9mA current in the reverse biased mode to the cell [refer]. The set up was disconnected and reconnected at 10-minute intervals to control the formation of focal heat. The whole process lasted for 60 minutes for each cell. An infrared (IR) camera was used for the hot spot detection in each cell during the reverse biasing. For the thermo-graphical analysis, Infrared ThermoCAM Pro 2.8 SR-3 spot meter software was used to locate the hot spot area/region, and marked. (For further details refer to [12-13]). The IR thermo-graphical analysis was done every 20 seconds to check for hot spot formation. The IR investigation shows that only one cell each from both technologies was found to develop hot spot formation after the reverse bias process. Two regions were marked from each cell, one from the affected region and the non-affected region. Figure 1 below shows the block diagram of the experimental setup illustrating how the cells were reverse bias duration the experimental process.

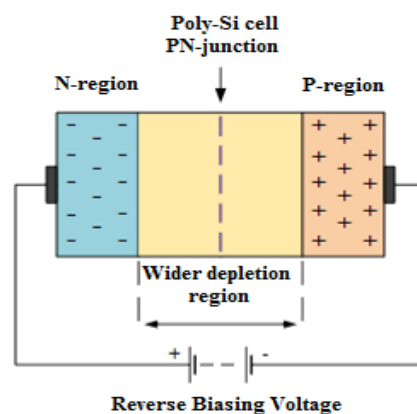


Fig. 1. Illustrates how the cells were reverse bias duration the experimental process.

## 2.2 Sample preparation

Immediately after locating the hot spot regions, the next stage was the sample preparation. In this stage, the following materials were used: a corrugated cardboard (larger than the size of the solar cell), straight edge (metal ruler), cutting glass tools (tungsten carbide scraper blade) and a jig. The jig was used for holding the cell during cutting in the case of mono-Si cell, for poly-Si cell no jig is required due to the fragile nature of the device. Each of the cells was placed on the corrugated cardboard and a masking tape was used to hold the sample while the metal ruler was placed on the cell to aid the process and for instituting uniform force distribution across the device. A sharp tungsten blade was used to meticulously cut out the required regions. For the mono-Si cell, a jig was used to hold the cell during cutting [15]. For clarity, the sample's areas cuts were larger than the region earlier marked during the IR analysis to ensure that the properties of the regions are not affected, as a result of the cuts

## 2.3 Fourier Transform Spectroscopy (FTIR)

Two samples were carefully prepared, one for the affected region and the other from the non-affected region. A non-flammable moisture free and quad filtered (easy duster) compressed air was used to clean the sample surface and placed under a closed sample holder. These samples were analyzed using, Fourier transforms infrared spectroscopy (FTIR) in the frequency range 660 to 4000 $\text{cm}^{-1}$ , to study the effect of hot spot formation on the absorbance of PV cells. The optical absorption and transmission spectrum of the two different PV technologies were examined. All the samples were analyzed, and the FTIR spectra patterns were obtained.

The FTIR operational principle is defined by the ability of the interferometer to generate an interferogram (signal) which is recorded by the infrared detector. The resulting spectrum (S) is derived from the Fourier transform interferogram, and this depends on the frequency ( $\nu$ ). The intensity of S depends on the path difference (x); these relationships are well defined by equation 1 and 2:

$$S(\nu) = \int_{-\infty}^{+\infty} I(x) e^{+i2\pi\nu x} dx = F^{-1}[I(x)] \quad (1)$$

$$I(x) = \int_{-\infty}^{+\infty} S(\nu) e^{+i2\pi\nu x} d\nu = F[S(\nu)] \quad (2)$$

where S is the spectrum, I is the signal (interferogram), x is the path difference between two beams. F is the Fourier and  $\nu$  is the frequency [16-17, 21].

## 3. Results and Discussion

### 3.1. Transmission spectral

Figs. 2 and 3 below show the transmission spectra for Poly-Si and Mono-Si respectively. These figures reveal the discrepancies between the intensities of the spectra from both the affected and non-affected region. The intensity of each peak depended on the vibrational frequency, which corresponds to the bonding nature in that region [14, 20, and 22]. In figure 2 for instance, the most dominating peaks corresponded to the following wave numbers: 676, 1013, 1524, 1688, 2092, 2248, 2341, 2923, 3615, 3738, and 3853  $\text{cm}^{-1}$ , while the highest is at 2341  $\text{cm}^{-1}$ . These peaks represent those bonds that are photon active in nature; hence their vibration frequencies correspond to the incident photon frequencies. There are three faint transmission peaks in the affective-region, which are absent in the non-affected region. These are attributed to the intermediate bond formation of weak bond energy. These peaks are located at 2092, 2248 and 2923  $\text{cm}^{-1}$  Wave numbers. The above peaks correspond to the presence of  $\text{C}\equiv\text{C}$  bond,  $-\text{N}=\text{C}=\text{O}$  disubstituted bond and C-H bond [18-19]. For the Mono- Si the highest peaks correspond to the following wave

numbers: 923, 2363, 683, 2925, 2122, 1556, 3842  $\text{cm}^{-1}$  respectively. The doublet broad peaks around 2550-2660  $\text{cm}^{-1}$ , which was found in the non-affected region only, is attributed to the presence of an S-H bond [20].

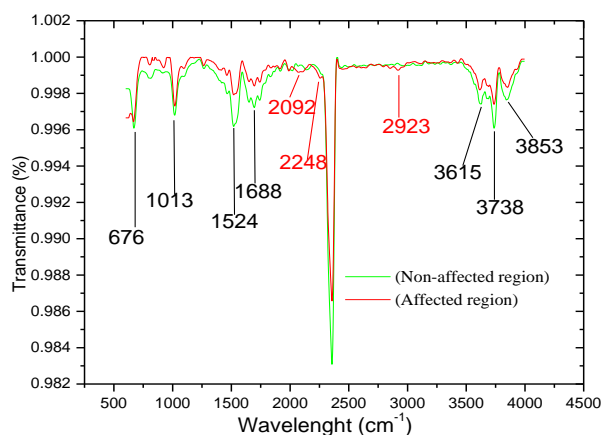


Fig. 2. FTIR spectra showing the transmission for Poly-Si cell both for the non-affected and the affected region

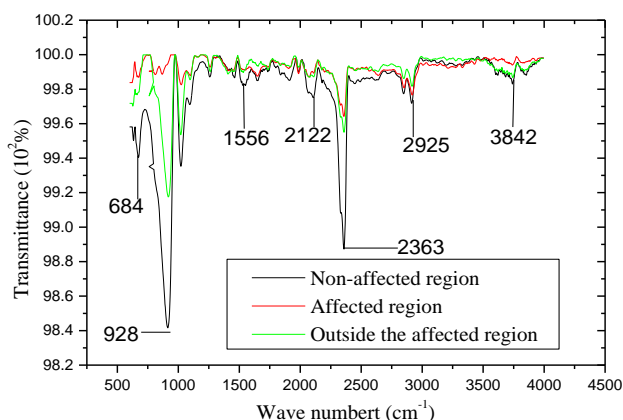


Fig. 3. FTIR spectra showing the transmission for Mono-Si cell both for the non-affected and the affected region

### 3.2. Absorption spectral

Figs. 4, 5 and 6 show the absorption spectra for Poly-Si and Mono-Si cells respectively. The results show that the optical behavior of Poly-Si spectra for the affected and non-affected regions have a more similar pattern when compared to that of a Mono-Si cell. Hence, three absorption spectra are shown for Mono-Si, while a single spectral is shown for the Poly-Si cell (Figure 4). Figure 4 shows some distinctive peaks around the following frequencies: 626, 1541, 2791, 3755  $\text{cm}^{-1}$ . At these wavenumbers (frequencies), the optical band spectral for the affected region is less than its corresponding non-affected region. At 915  $\text{cm}^{-1}$  wave number, the affected spectral is slightly more than its corresponding non-affected spectral. The sharp medium stretch band at 2597  $\text{cm}^{-1}$  is absent from the non-affected region. In general, the optical spectral of the Poly-Si cell is similar in both regions unlike the Mono-Si cell.

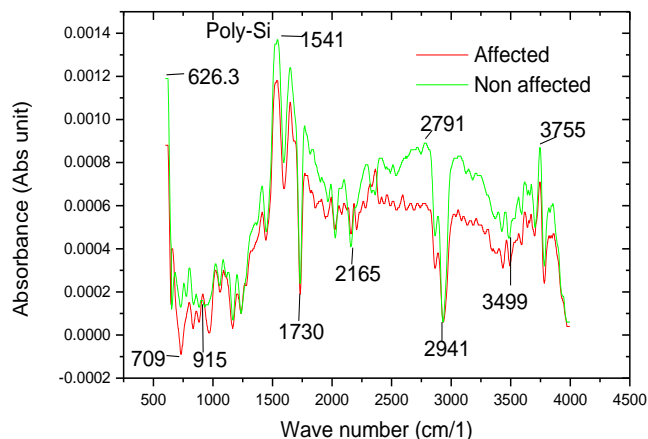


Fig. 4. FTIR spectra for Poly-Si cell showing the absorption for both the non-affected and affected region

For the Mono-Si cell, three distinct sections can be observed as shown in Fig. 5. These sections are: A (black), B (blue) and C (pink). In section A, there is no similarity between the spectral pattern for both the non-affected and affected region. There are strong absorption peaks at the following frequencies: 3606, 3754 and 3870  $\text{cm}^{-1}$  for the non-affected region. Where section B is characterized by the presence of weak overtones (peaks) for both regions. However, in section C, the intensity of absorption bands is stronger and sharper than in section B. In addition, three different areas were analyzed for Mono-Si, for a better understanding of its absorption spectral. The analyzed areas include; the finger line, spot outside the grain boundary and the grain boundary spot. These were done for both the affected and non-affected region. The results are presented in figures 6, 7 and 8. These analyses help to demonstrate the disparity in the absorption behaviour along various spots in Mono-Si solar cell.

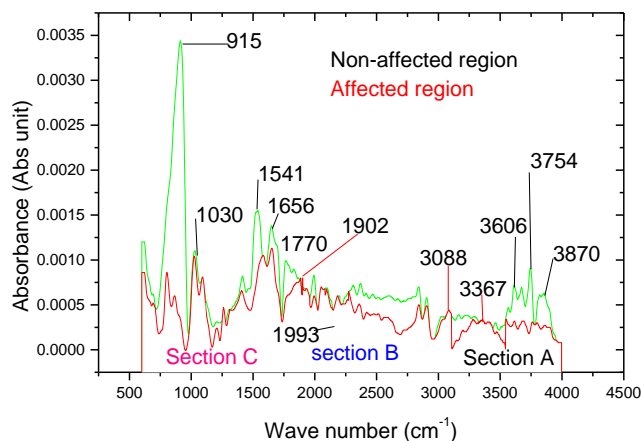


Fig. 5. FTIR spectra for Mono-Si cell showing the absorption for both the non-affected and the affected region

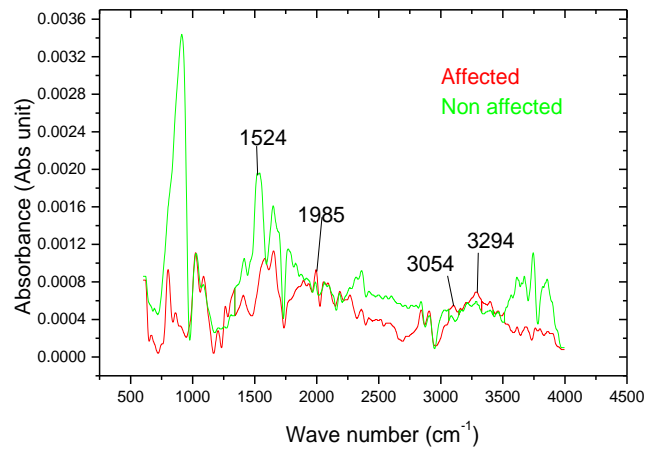


Fig. 6. FTIR spectra for Mono-Si cell showing the relationship of the spectra from non-affected region and affected through the grain

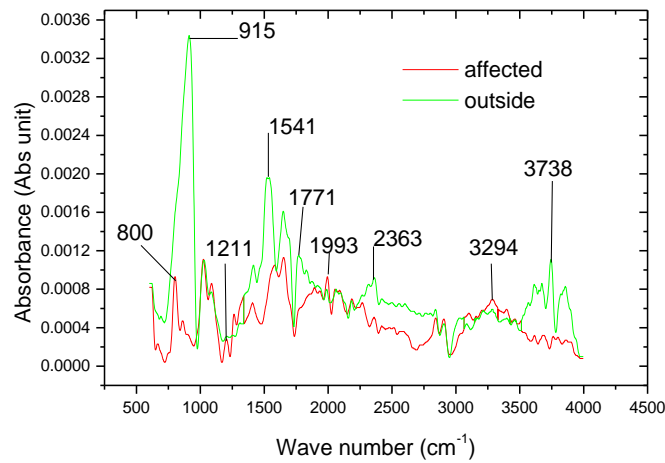


Fig. 7. FTIR absorption spectral for Mono-Si showing the non-region region and the affected region outside the grain boundary

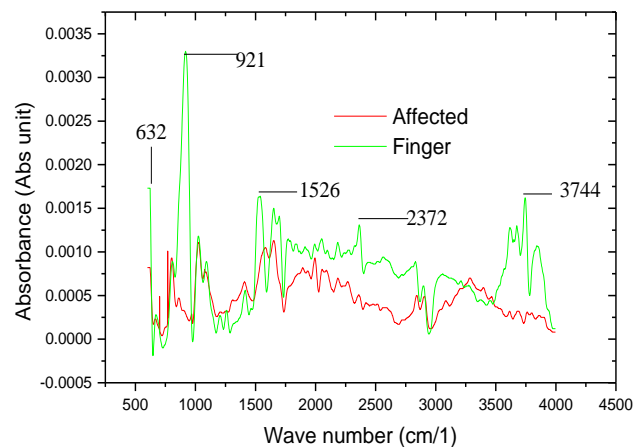


Fig. 8. FTIR absorption spectral for Mono-Si showing the non-region region and the affected region outside the grain boundary from the finger line for Mono-Si cell

### 3.3 Optical spectral quantitative analysis

Statistical analysis was used to quantify the optical density spectra, which are absorbed into the non-affected and affected region. The percentage difference was used as the analytical tool. These indicate the percentage difference between the amounts of the photon absorbed by each

region. It is important to note that only the optical band of strong intensity, from each section as stated in Figures 2, 3, 4 and 5 are used. The results are presented in Figures 9 and 10. For the Poly-Si cell shown in Figure 9, the reduction in the quantity of incident photon absorption in the normal region compared to the affected region is within 55% to 11%, with the highest loss in the region of  $900\text{ cm}^{-1}$  and  $2700\text{--}3100\text{ cm}^{-1}$  wave numbers. Figure 10 shows the amount of optical loss resulting from the localized heating for a Mono-Si cell. Approximately 91% of the incident photons are lost around  $980\text{ cm}^{-1}$ , while there is a 81% reduction of the photon close to the  $3600\text{ cm}^{-1}$  wave number. The lowest lost record is about 22%. This implies that Mono-Si cell absorbent layer is more prone to absorption degradation during hot spot formation than Poly-Si, at frequency range of  $880\text{--}920\text{ cm}^{-1}$  and  $3600\text{--}3800\text{ cm}^{-1}$ .

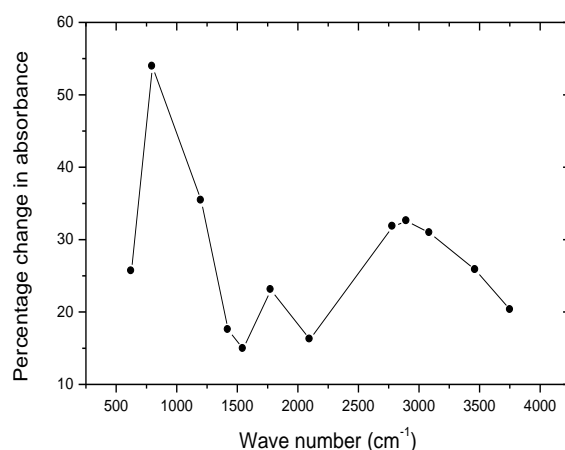


Fig. 9. Percentage change in the absorption spectral for Poly-Si cell due to hot spot formation

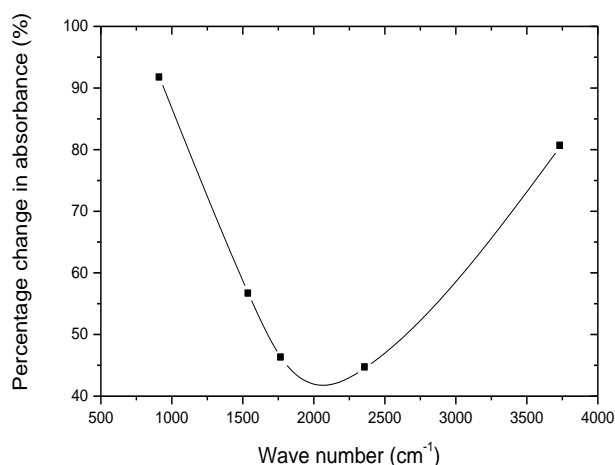


Fig. 10. Percentage change in the absorption spectral for Mono-Si due to hot spot formation

#### 4. Conclusion

This study revealed that the presence of localized heating which leads to hot spot formation has a negative effect on Poly-Si and Mono-Si solar cells. Hot spot formation has diverse effects on different solar technologies as can be seen in Figures 9 and 10. The percentage loss in absorbance by the Poly-Si differs from the percentage loss by the Mono-Si. This does not mean that the Poly-Si is a better-performing cell than the Mono-Si but it simply means that both cells exhibit various degrees of hot spot formation.

Since it is exclusively the photon which has been absorbed that contributes to recombination, the degradation revealed in this experiment is entirely due to absorption

degradation. Hot spot formation directly decreases the absorbance of the cell. The significance of this finding helps provide a better understanding of the extent of the damage that localized heating causes to solar cell optical absorption. This will enable researchers to develop a better model that can optimize light intake and optical confinement, even in the presence of hot spot formation.

### Acknowledgements

We sincerely thank Mcako Thandisile of the University of Fort Hare University, chemistry department for his invaluable laboratory assistance. Lastly, the authors wishes to thank Eskom for financing this project.

### References

- [1] A. Richter, M. Hermle, S. W. Glunz, *IEEE Journal of Photovoltaics* **4**, 1184 (2013).
- [2] M. Wolf, Historical development of solar cells, *Proc. 25th Power Sources Symposium*, In *Solar Cells*, ed. C.E Backus, IEEE Press, (1976).
- [3] R. *et al*, William, *Journal of Applied Physics* (ISSN 0021-8979), **54**, 6721 (1983).
- [4] R. Santbergen, R. J. C. van Zolingen, *Solar Energy Materials & Solar cells*, (2007).
- [5] W. Shockley, H. J. Queisser, *Journal of Applied physics*, doi: 10.1063/1.1736034, **32**, 510 (1961).
- [6] L. C. Hirst, N. J. E. Daukes, Fundamental losses in solar cells, available online (<https://workspace.imperial.ac.uk/quantumphotovoltaics/public/Hirst-EUPVSEC24>) (2008).
- [7] F. Dinçer, M. E. Meral, Critical factors that affecting efficiency of solar cells ,*Smart Grid and Renewable Energy*, access online (<http://www.SciRP.org/journal/sgre>) **1**, 47-50 (2010).
- [8] E. I Meyer and E. E Van Dyk. Reliability and Degradation of Photovoltaic Module Performance Parameters. *IEEE*, **53**, 1, 83 (2004).
- [9] W. William, Absorption of electromagnetic radiation” in *Access Science*, McGraw-Hill Education, available on <http://www.accessscience.com>, (2012).
- [10] T. Olav, *Elementry Physics of P-N Junction*, (2007).
- [11] P. M. A. Sherwood, *Vibrational spectroscopy of solids*, Cambridge University press, U.k, (1972).
- [12] G. O Osayemwenre, The electrical, structural and elemental degradation of Single junction amorphous silicon modules. A dissertation submitted in fulfillment of the requirements for Master degree in Physics at University of Fort Hare Alice, South Africa (2013).
- [13] M. Simon, On the evaluation of spectral effects on PV modules performance parameters and hot hot-spot in solar cells, A thesis submitted in fulfillment of the requirements for the degree of Doctor of Philosophy in Physics at University of Fort Hare Alice, South Africa (2008).
- [14] O. Schnepf, *Theory for the infrared absorption intensities of the lattice*, (1967).
- [15] E. F. Thomas, C. J. Vierck, *Engineering Drawing and Graphic Technology*, Eleventh Edition. **621–624**, accessed online from [www.schematic-diagram.ru](http://www.schematic-diagram.ru) (1975).
- [16] T. Hirschfeld, Optical microscopic observation of single small molecules, *Appl Optics* available online at <http://dx.doi.org/10.1364/AO.15.002965> **15**, 2965-2966, (1976).
- [17] N. Jaggi and D.R. Vij, *Fourier Transform Infrared Spectroscopy*, *Fourier handbook*, accessed 10/07/2014 online at <http://pcwww.liv.ac.uk>.
- [18] J. Rosaleen, D. Anderson, J. Bendell, W. P. Groundwater, *Organic Spectroscopic analysis*, The royal society of chemistry, 2nd ed., 27-50 (1987).
- [19] B. George, P. McIntyre, *Infrared Spectroscopy (Analytical chemistry)* **72**, 190 (1987).
- [20] G. Randall, E. George, S. Kriz, G. M. Lampman, D. L. Pavia, *Introduction to organic laboratory techniques*, revised edition, (2011).
- [21] P. Hoffmann, E. Knozinger, *Appl. Spectroscopy*. **41**, 1303-1306 (1987).
- [22] Z. H. Lu, Q. Yao, Energy analysis of silicon solar cell modules based on optical model for arbitrary layers”, *Solar Energy* **18**, 636 (2007).